Journal of Controlled Release 286 (2018) 33–45

Contents lists available at ScienceDirect

Journal of Controlled Release

journal homepage: www.elsevier.com/locate/jconrel

Connecting the *in vitro* and *in vivo* experiments in electrochemotherapy - a feasibility study modeling cisplatin transport in mouse melanoma using the dual-porosity model

Janja Dermol-Černe[a], Janja Vidmar[b], Janez Ščančar[b], Katja Uršič[c], Gregor Serša[c,d], Damijan Miklavčič[a,*]

[a] University of Ljubljana, Faculty of Electrical Engineering, Tržaška cesta 25, 1000 Ljubljana, Slovenia
[b] Jozef Stefan Institute, Department of Environmental Sciences, Jamova cesta 39, 1000 Ljubljana, Slovenia
[c] Institute of Oncology Ljubljana, Department of Experimental Oncology, Zaloška cesta 2, 1000 Ljubljana, Slovenia
[d] University of Ljubljana, Faculty of Health Sciences, Zdravstvena pot 5, 1000 Ljubljana, Slovenia

ARTICLE INFO

Keywords:
Electrochemotherapy
Drug delivery
Transport
Modeling
Dual-porosity model

ABSTRACT

In electrochemotherapy two conditions have to be met to be successful – the electric field of sufficient amplitude and sufficient uptake of chemotherapeutics in the tumor. Current treatment plans only take into account critical electric field to achieve cell membrane permeabilization. However, permeabilization alone does not guarantee uptake of chemotherapeutics and consequently successful treatment. We performed a feasibility study to determine whether the transport of cisplatin *in vivo* could be calculated based on experiments performed *in vitro*. *In vitro*, a spectrum of parameters can be explored without ethical issues. Mouse melanoma B16-F1 cell suspension and inoculated B16-F10 tumors were exposed to electric pulses in the presence of chemotherapeutic cisplatin. The uptake of cisplatin was measured by inductively coupled plasma mass spectrometry. We modeled the transport of cisplatin with the dual-porosity model, which is based on the diffusion equation, connects pore formation with membrane permeability, and includes transport between several compartments. In our case, there were three compartments - tumor cells, interstitial fraction and peritumoral region. Our hypothesis was that *in vitro* permeability coefficient could be introduced *in vivo*, as long as tumor physiology was taken into account. Our hypothesis was confirmed as the connection of *in vitro* and *in vivo* experiments was possible by introducing a transformation coefficient which took into account the *in vivo* characteristics, *i.e.*, smaller available area of the plasma membrane for transport due to cell density, presence of cell-matrix *in vivo*, and reduced drug mobility. We thus show that it is possible to connect *in vitro* and *in vivo* experiments of electrochemotherapy. However, more experimental work is required for model validation.

1. Introduction

When biological cells are exposed to short high-voltage pulses, the permeability of the cell membrane increases, presumably due to pore formation following electroporation. As a result, membrane-impermeant molecules can pass the membrane [1–4], presumably through newly formed pores. If cells recover, electroporation is called reversible. If the damage is too severe and cells die, electroporation is called irreversible. Electroporation is used in biotechnology [5], food processing [6, 7] and medicine [8, 9], *e.g.* electrochemotherapy [10, 11], gene electrotransfer [12, 13], irreversible electroporation as an ablation technique [14, 15] and transdermal drug delivery [16, 17].

In electrochemotherapy, transport of chemotherapeutics is critical for a successful treatment. In standard electrochemotherapy treatment, after intravenous or intratumoral injection of chemotherapeutic delivered electric pulses enhance the uptake of chemotherapeutics into tumor cells [18–20]. In electrochemotherapy, chemotherapeutics cisplatin and bleomycin are commonly used as described in the Standard Operating Procedures [19, 21]. Starting in the late 1980s [22–24] with preclinical experiments, followed by clinical studies [25, 26], intratumoral injection of cisplatin was introduced into the Standard Operating Procedures of the electrochemotherapy [19] and is now a well-established therapy in clinics across Europe [10, 11]. Cisplatin enters cells by passive (diffusion) as well as active (endocytosis, pinocytosis, macrocytosis, membrane transporters) mechanisms [27–29]. Tumor cells can become resistant to cisplatin due to several mechanisms;

* Corresponding author.
E-mail address: Damijan.miklavcic@fe.uni-lj.si (D. Miklavčič).

https://doi.org/10.1016/j.jconrel.2018.07.021
Received 22 December 2017; Received in revised form 9 July 2018; Accepted 13 July 2018
0168-3659/ © 2018 Elsevier B.V. All rights reserved.

modified transport or detoxification, or increased DNA damage repair [29]. However, if the mechanism of resistance depends on membrane restriction of cisplatin uptake or increased pumping out of the cell, the resistant and non-resistant cells were shown to respond similarly to electroporation *in vitro* [30]. The situation *in vivo* was different, as electroporation was more effective on parental than cisplatin-resistant tumors, and it can only be hypothesized that additional factors could be present. Cisplatin is known to have negative side effects, among them nephrotoxicity, ototoxicity, nausea, depending on the cisplatin concentration and administration of the drug [31]. When injected, it accumulates in different organs (blood, liver, kidneys, brain) [32]. Electrochemotherapy offers a possibility to deliver lower dose than in chemotherapy while increasing local effectiveness. When treating patients with electrochemotherapy, we can follow the Standard Operating Procedures where electrode geometry, parameters of electric pulses, chemotherapeutic dose, and administration route are predefined [19, 21]. When tumors are outside the standard parameters, we can use variable electrode configuration [33]. With variable electrode configuration, we need a treatment plan where the position of the electrodes and electric pulse parameters are optimized to offer sufficient tumor coverage with above-threshold electric field [34–38]. Current treatment planning procedure could be upgraded by introducing a model of transport to the treatment plan. In this case, the spatially and temporally dependent number of intracellular cisplatin molecules could be calculated. Number of bleomycin molecules which must enter the cell to cause cell death has already been determined to be a few thousand [39]. If a similar dependency, *i.e.*, a necessary number of internalized molecules to cause cell death, would also be revealed for cisplatin, treatment efficacy could be more precisely predicted.

Usually, experiments are first performed *in vitro* and then translated to *in vivo*. However, it is difficult to compare the transport during electroporation *in vivo* and *in vitro*. In *in vitro* experiments with single cell suspensions, the solute surrounds the cells, and the transport of solute occurs via diffusion. Solute can pass cell membrane where the membrane is permeabilized. The transport in the extracellular space is not limited. If there is enough of solute in the extracellular space, the transport stops when a cell membrane reseals after electroporation. The transport through the membrane can be directly linked to cell membrane permeability [40]. *In vivo*, the initial solute concentration varies spatially. All the solute available can enter cells before the membrane reseals and although cell membrane is still permeable, it does not enter cells anymore, *i.e.*, the extracellular compartment can be locally depleted [41]. The transport of solute occurs via diffusion and convection [42]. Cells are close together which decreases the possible area for the uptake and decreases the induced transmembrane voltage due to electric field shielding [41]. Already in spheroids, it was shown that transport of small molecules was spatially heterogeneous, cells inside the spheroid contained less of solute than cells at the rim of the spheroid due to established concentration gradient [42, 43]. Electric pulses cause vasoconstriction [44] which limits the transport of solute in or out of a tumor and prolongs its exposure to chemotherapeutic. In a tumor, increased interstitial pressure, heterogeneous perfusion, defective lymphatic circulation, binding of the drug to non-target molecules and metabolism additionally affect the transport [45–48].

Modeling is advantageous since it decreases the number of necessary experiments and facilitates understanding of the underlying processes. Several models of the increased uptake of molecules after electroporation exist. For example, statistical models which describe the data well but do not include specific transport mechanisms [49], the kinetic scheme of electroporation [50, 51], (electro)diffusion through a permeable membrane or a single pore [52–56] and pharmacokinetic models [57, 58]. We, however, decided to use the dual-porosity model [40, 59] which is based on the diffusion equation, connects pore formation with membrane permeability, and includes transport between several compartments - in our case between the intracellular space, the interstitial tumor fraction and the peritumoral environment, and can also include thermal relations [60].

We focused on the electrochemotherapy and drug transport after delivery of electric pulses, *i.e.*, electroporation. We performed a feasibility study to determine whether it is possible to model drug transport *in vivo* based on the data obtained *in vitro*. Our hypothesis was that *in vitro* membrane permeability coefficients could be used to model the transport of cisplatin *in vivo*. We used chemotherapeutic cisplatin as its intracellular mass can be determined via measuring the mass of Pt by inductively coupled plasma mass spectrometry [61] which is a very sensitive and precise method. We exposed suspension of mouse melanoma cells to electric pulses in the presence of cisplatin and measured the intracellular mass of Pt. We used the dual-porosity model to calculate the *in vitro* permeability coefficient as a function of pulse number and electric field. We performed *in vivo* experiments on mouse melanoma tumors and measured the intracellular and extracellular Pt mass, the mass of Pt in the serum, the mass of Pt bound to the DNA and components other than the DNA (*i.e.*, proteins and lipids). We built a 3D numerical model of a tumor and by using the *in vitro* permeability coefficient calculated the mass of Pt in a tumor. We confirmed our hypothesis and determined that a transformation from *in vitro* to *in vivo* was possible by introducing a transformation coefficient which took into account the smaller available area of cell membrane for transport due to cell density, and presence of cell-matrix *in vivo*. Our model could describe the amount of intracellular Pt and Pt in the interstitial fraction in a mouse melanoma after electroporation. We show that the transport at the cell level (*in vitro*) could be connected with the tissue level (*in vivo*) and this connection could eventually be used in treatment planning. In future, however, different tumor types and drugs should be tested with our model to establish whether *in vitro – in vivo* connection is valid also under different experimental conditions than currently tested in our present study.

2. Materials and methods

2.1. In vitro experiments

2.1.1. Cell preparation

Mouse skin melanoma cell line B16-F1 was grown until 80% confluency in an incubator (Kambič, Slovenia) at 37 °C and humidified 5% CO_2 in Dulbecco's Modified Eagle's Medium (DMEM, cat. no. D5671, 13.77 mS/cm, 317–351 mOs/kg). The cell line was tested to be mycobacterium free. DMEM was supplemented with 10% fetal bovine serum (cat. no. F7524), 2 mM L-glutamine (cat. no. G7513) and antibiotics (50 μg/ml gentamycin (cat. no. G1397), 1 U/ml penicillin-streptomycin (cat. no. P11–010, PAA, Austria)) and was in this composition also used as electroporation buffer and for dilution of the samples.

The cell suspension was prepared by detaching the cells by 10× trypsin-EDTA (cat. no. T4174), diluted 1:9 in Hank's basal salt solution (cat. no. H4641). Trypsin was inactivated with the DMEM containing 10% fetal bovine serum. For electroporation, cells were centrifuged (5 min, 180 *g*, 21 °C) and resuspended in DMEM containing 10% fetal bovine serum at concentration 2.2×10^7 cells/ml. The chemicals were from Sigma Aldrich, Germany, unless noted otherwise.

2.1.2. Cell electroporation

The 3.3 mM stock cisplatin (Accord Healthcare, Poland) was diluted in 0.9% NaCl, according to the manufacturer's instructions, and prepared fresh for each experiment. Right before experiments, 120 μl of cell suspension was mixed with a required quantity of cisplatin to achieve the desired concentration (usually 100 μM, unless noted otherwise). 60 μl of the cell suspension was transferred between the 2 mm stainless-steel electrodes [62], and pulses were delivered with a commercially available BetaTech electroporator (Electro cell B10, BetaTech, France). We varied the pulse number (1, 4, 8, 16, 32, 64) and the electric field (0.4 kV/cm, 0.6 kV/cm, 0.8 kV/cm, 1.0 kV/cm, 1.2 kV/

cm) while pulse duration was 100 μs and repetition frequency 1 Hz. The remaining 60 μl was used as a control and was transferred between the electrodes, but no pulses were delivered. 50 μl of the treated and control sample was transferred into 15 ml centrifuge tubes. 10 min after pulse delivery (unless noted otherwise), the samples were diluted 40 × in full DMEM and vortexed. Samples were then centrifuged (5 min, 900 *g*, 21 °C) and the supernatant was separated from the pellet. Until the Pt mass measurements, the samples were stored at −20 °C.

The following parameters were tested during establishement of our protocol: 1) the effect of extracellular cisplatin (1 μM, 5 μM, 10 μM, 20 μM, 50 μM, 100 μM, 200 μM, 330 μM) on the intracellular Pt mass 2) time interval (5 min, 10 min or 20 min) between pulse delivery and dilution on the intracellular Pt mass, 3) the binding of cisplatin to proteins from fetal bovine serum by using DMEM with or without fetal bovine serum as the electroporation buffer, 4) we also determined the resealing time by adding 100 μM cisplatin 2 min, 5 min, 10 min and 20 min after pulse delivery. In the experiments mentioned in this paragraph, 8 × 100 μs pulses at 1.0 kV/cm and 1 Hz repetition frequency were delivered.

2.1.3. Cell death - irreversible electroporation

Survival after electroporation (without cisplatin) was assessed with two different assays. Short-term irreversible electroporation was measured 1 h after the treatment on flow cytometer by the propidium iodide uptake. The long-term irreversible electroporation was measured 24 h after the treatment by a metabolic assay. Cells were prepared the same way as described under Cell preparation. Electroporation was performed as described in Cell electroporation section, but we added 0.9% NaCl instead of cisplatin.

2.1.3.1. Short-term irreversible electroporation. After application of electric pulses, cells were incubated at 37 °C for 30 min. During these 30 min cells resealed. We added propidium iodide (Life Technologies, USA) in final concentration 136 μM. As reversibly electroporated cells were already resealed, only irreversibly electroporated cells stained. After 5 min in the propidium iodide, we measured fluorescence on the flow cytometer (Attune NxT; Life Technologies, USA). Cells were excited with a blue laser at 488 nm, the emitted fluorescence was detected through a 574/26 nm band-pass filter, and 20.000 events were acquired. Two distinct peaks were formed on the histogram of fluorescence and percentage of dead cells was determined with Attune NxT software (Life Technologies, USA).

2.1.3.2. Long-term irreversible electroporation. Long-term death was assessed 24 h after electroporation with the MTS test (CellTiter 96® AQueous One Solution Cell Proliferation Assay (MTS), Promega, USA). 20.000 cells per well were transferred into in a 96-well plate in triplicates and then incubated for 24 h. 20 μl of the MTS was added per well, and after 2 h at 37 °C, the absorbance at 490 nm was measured with a spectrofluorometer (Tecan Infinite 200; Tecan, Austria).

2.2. Statistical analysis

The statistical analysis was performed in SigmaPlot (v11.0, Systat Software, USA). We performed the *t*-test when the normality test passed, or the Mann-Whitney rank sum test when the normality test failed.

2.3. In vivo experiments

In the *in vivo* experiments, part of the experimental data was reused [63] (mass of the Pt 60 min after the treatment). We additionally performed experiments where we determined the mass of the Pt 2 min after injection which corresponds to the time-point when electric pulses were applied to determine the initial conditions of our model.

2.4. Animals

Eight-week-old female C57Bl/6 mice (Envigo Laboratories, Udine, Italy) were used in experiments. At the beginning of the experiments, their body weight was between 18 and 20 g. All procedures were performed in compliance with the guidelines for animal experiments of the EU Directives, the permission of the Ministry of Agriculture and the Environment of the Republic of Slovenia (Permission no. U34401–1/2015/16), which was provided based on the approval of the National Ethics Committee for Experiments on Laboratory Animals. Mice were kept in a specific pathogen-free environment with 12-h light/dark cycles at 20–24 °C with 55% ± 10% relative humidity and given food and water *ad libitum*.

2.5. Treatment and sample collection protocol

One day before the experiment, mice were shaved on their right flank. Tumors were induced in the right flanks of the non-anesthetized mice with subcutaneous inoculations of 10^6 B16-F10 melanoma cell suspensions in 100 μl of a physiological solution prepared from cell culture *in vitro*. The treatment was performed 6–7 days post-inoculation when tumors reached volumes of 35–40 mm^3. Tumor volume was measured using a vernier caliper. The tumor volume was calculated using the following formula:

$$V = \pi \times e_1 \times e_2 \times e_3 \div 6 \quad (1)$$

where e_1, e_2, and e_3 are three orthogonal diameters of the tumor [63]. During the treatment, mice were under isoflurane (Izofluran Torrex para 250 ml, Chiesi Slovenia, Ljubljana, Slovenia) anesthesia. To obtain precise application of electroporation mice were initially anesthetized with inhalation anesthesia in the induction chamber with 2% (v/v) of isoflurane in pure oxygen and afterward, the mouse muzzle was placed under inhalation tube to keep mice anesthetized during the experiment. In experiments from [63], mice were randomly divided into three experimental groups, consisting of three animals per group. The three groups were: 1) control group, where we intratumorally injected 80 μl of physiological solution, 2) cisplatin group, where we injected 80 μl of cisplatin (40 μg of cisplatin) and 3) cisplatin and electroporation group, *i.e.* electrochemotherapy, where we injected 80 μl of cisplatin (40 μg of cisplatin) and after 2 min delivered electric pulses. Pt mass in these three groups was determined 60 min after injection as described in [63].

In the scope of this paper, additional two groups were used with three mice per group. The treatment consisted of an intratumoral injection of 80 μl cisplatin (40 μg of cisplatin). After two minutes, tumors were excised, removed from the overlying skin and weighted. The blood was collected from the intraorbital sinus using glass capillary tubes. In the first group, we measured Pt in a whole tumor, and in the second group, Pt in several tumor compartments (serum, single cell suspension, extracellular matrix, DNA) [63]. For total tumor Pt content detection, tumors were frozen at −20 °C until analysis was performed.

2.6. Platinum measurements

For Pt determination inductively coupled plasma mass spectrometry (ICP-MS) was used.

2.6.1. Sample digestion

All dilutions of the samples were made with ultrapure water (18.2 MΩ cm) obtained from a Direct-Q 5 Ultrapure water system (Merck Millipore, USA). Nitric acid (65% HNO_3) and hydrogen peroxide (30% H_2O_2) were obtained by Merck Millipore, USA.

Samples of cell pellet were digested with 200 μl of concentrated nitric acid, 200 μl of concentrated hydrogen peroxide and heated overnight at 90 °C in the heating oven (Binder GmbH, Tuttlingen, Germany). After the digestion, the samples were filled up to 5 ml with

MilliQ water and measured by ICP-MS.

Samples of supernatant fluid were digested with one ml of concentrated nitric acid, one ml of concentrated hydrogen peroxide and heated overnight at 90 °C in the heating oven. After the digestion, the samples were filled up to 10 ml with MilliQ water and 2.5-times diluted before ICP-MS measurements.

Samples from the *in vivo* experiments were digested at 90 °C for approximately 36 h in 0.2 to 2.0 ml of a mixture of concentrated nitric acid and hydrogen peroxide (1:1). After obtaining clear solutions, samples were adequately diluted with MilliQ water before ICP-MS measurements.

2.7. Inductively coupled plasma – mass spectrometry measurements

Mass concentrations of Pt in the digested samples were determined by the use of mass spectrometry with inductively coupled plasma (ICP-MS) against an external calibration curve using Ir as an internal standard. Calibration standard solutions of Pt were prepared from Pt stock solution (1000 μg Pt/ml in 8% HCl), obtained from Merck (Darmstadt, Germany), and diluted in 2.6% nitric acid. Experimental conditions for the ICP-MS instrument (Agilent 7900 ICP-MS instrument, Agilent Technologies, Tokyo, Japan), summarized in Table 1, were optimized for plasma robustness and adequate sensitivity.

For evaluation of the accuracy of the analytical method (digestion procedure and ICP-MS analysis), the same quantity of cell pellet was spiked with 20 μl of 500 ng/ml ionic Pt solution to reach final Pt concentration of 10 ng/sample, while the supernatant fluid was spiked with 20 μl of 50 μg/ml ionic Pt solution to reach final Pt concentration of 1000 ng/sample. Spiked samples were digested in the same way as described before. Recoveries (the ratio between the measured and expected Pt concentrations) were 101 ± 2% ($N = 4$) and 98 ± 1% (N = 4) for spiked cell pellets and spiked supernatant fluids, respectively.

2.8. Modeling

2.8.1. In vitro

From the *in vitro* results, we calculated the coefficient of membrane permeability to Pt (P). *In vitro*, the model of transport was relatively simple – the initial concentration of the extracellular cisplatin was the same for all the cells, there was enough of cisplatin so that we could consider the extracellular cisplatin concentration constant. The whole cell was surrounded by cisplatin which could enter from all sides, depending on the permeability of the membrane. By changing the pulse number and voltage, we obtained the permeability coefficient as a function of pulse number and electric field intensity. Permeability coefficient was a direct measure of membrane permeability.

Table 1
ICP-MS operating parameters for determination of elements.

Parameter	Type/Value
Sample introduction	
Nebulizer	Micromist
Spray chamber	Scott
Skimmer and sampler cone	Ni
Plasma condition	
Forward power	1550 W
Plasma gas flow	15.0 l/min
Carrier gas flow	1.05 l/min
Nebulizer pump	0.1 rps
Sample depth	8.0 mm
He gas flow	0 ml/min
Energy discrimination	5.0 V
Data acquisition parameters	
Isotopes monitored	^{195}Pt
Isotopes of internal standards	^{193}Ir

The resealing time constant was determined by describing the resealing data with a curve:

$$f(t) = C\exp\left(-\frac{t}{\tau}\right) \tag{2}$$

Where C denotes the intracellular Pt mass if cisplatin is present at the moment of pulse delivery, τ is the resealing time constant or time when 63% of the pores/defects are resealed [64], and t is the time elapsed since the end of pulse delivery.

In vitro, we used the dual-porosity model [40] to calculate the permeability coefficient. In Matlab (R2017a, Mathworks Inc., USA) we calculated the permeability coefficient (P) at $t = 0$ s which corresponds to P_0 by solving the differential equation:

$$\frac{\partial c_{int}}{\partial t} = P_0\exp\left(-\frac{t}{\tau}\right)\frac{3}{R}(c_{int} - c_{ext}) \tag{3}$$

for the external concentration c_{ext} (100 μM), the resealing constant τ (2.29 min), *in vitro* cell radius R (8.1 μm) [65], and initial conditions $c_{int}(t = 0\text{ s}) = 0$ μM. The permeability coefficient was a function of time as the permeability decreased with time due to membrane resealing.

2.8.2. In vivo

Model of a tumor was constructed in Comsol Multiphysics® (v5.3, Comsol AB, Stockholm, Sweden). The tumor was modeled as a sphere with radius 2.03 mm which corresponds to 35 mm^3, *i.e.*, the average volume of a tumor when the *in vivo* treatment was performed. Assuming spherical symmetry, we modeled only 1/8 of the tumor, *i.e.*, one octant of the sphere (photo of a tumor is available in the Supplemental Material). We used physics-controlled mesh with extra fine element size and confirmed that with decreasing element size, the calculated intra- and extracellular Pt mass did not change significantly. In Comsol, two equations were coupled and calculated in a whole tumor. In the intracellular space:

$$\frac{\partial c_{int}}{\partial t} = -\frac{3P(t)}{R}(c_{int} - c_{ext})k \tag{4}$$

And in the extracellular space:

$$\frac{\partial c_{ext}}{\partial t} = D_{cddp}\nabla^2 c_{ext} + \frac{3P(t)}{R}\frac{(1-f)}{f}(c_{int} - c_{ext})k \tag{5}$$

Where c_{int} and c_{ext} denote the intracellular and extracellular concentration, respectively, D_{cddp} is the diffusion coefficient of cisplatin in the extracellular tumor space, P is the permeability coefficient, time-dependent due to membrane resealing, R is the cell radius *in vivo* (6.25 μm) [66], f is the fraction of cells in a tumor (37%) [66, 67], and k is the transformation coefficient which transforms the data from the *in vitro* to the *in vivo* conditions. The initial conditions were $c_{int}(t = 0) = 0$ mM and $c_{ext}(t = 0) = 1.6$ mM. P was determined in the *in vitro* experiments. The boundary conditions for the intracellular concentration were no flux on all boundaries and for extracellular concentration, no flux in the inner boundaries of a tumor and $c_{ext}(r = 2.03\text{ mm}) = 0$ mM at external boundaries.

In a model, we varied parameters k and D_{cddp} and calculated the intracellular and extracellular Pt mass for each combination of k and D_{cddp} when k was between 0 and 1 in steps of 0.2 and D_{cddp} was between 2×10^{-8} cm^2/s and 8×10^{-5} cm^2/s in steps of 0.2 decades. Then, we determined a global minimum and sampled the space around it with higher resolution by changing k from 0.3 to 0.5 by 0.1 and D_{cddp} from 1.5×10^{-6} cm^2/s to 2.5×10^{-6} cm^2/s by 0.1 decades. The final values of the parameters k and D_{cddp} were chosen as the values with which we achieved the best agreement with a measured mass of Pt *in vivo* and were the global minimum.

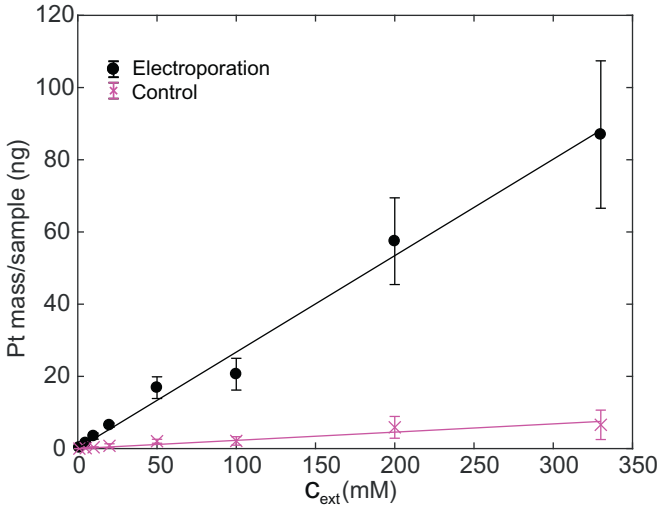

Fig. 1. Effect of extracellular cisplatin (C_{ext}) concentration on intracellular Pt mass when 8 × 100 μs pulses of 1 kV/cm were delivered at repetition frequency 1 Hz (mean ± standard deviation). The results could be fit well with a linear function $y = kc_{ext}$with k and R^2 of 0.2672 and 0.99 for the treated and 0.0228 and 0.92 for the control cells, respectively. Each data point was repeated 3–5 times. Except for 1 μM extracellular cisplatin where the measured values were below the detection threshold of 0.005 ng and we could not evaluate statistical significance, all electroporated samples were statistically different from the corresponding control samples ($P \leq 0.03$).

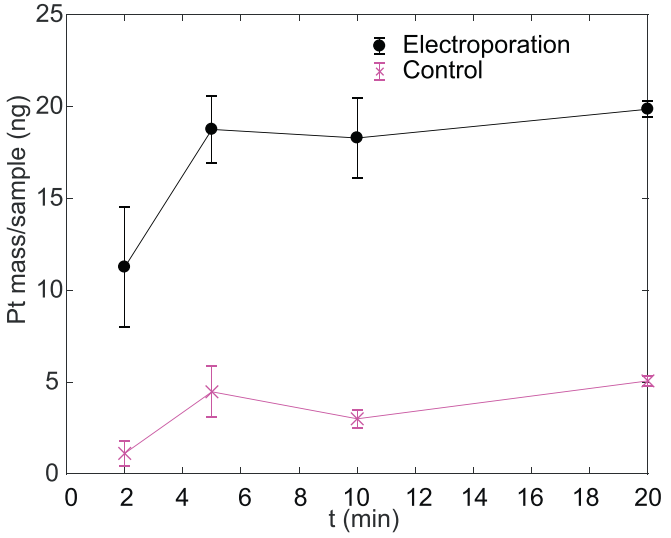

Fig. 2. Effect of incubation time after pulse application on the intracellular Pt mass when 8 × 100 μs pulses of 1 kV/cm were delivered at repetition frequency 1 Hz and 100 μM extracellular cisplatin (mean ± standard deviation). Already 5 min after pulse delivery a plateau was reached. Each data point was repeated 3–6 times. All treated samples were statistically different from the corresponding control ($P \leq 0.001$). There was a significant difference between 2 min and 5 min exposure of treated samples ($P = .02$), other comparisons were not significant.

3. Results

3.1. In vitro experiments

First, we performed experiments to determine the effect of extracellular cisplatin concentration, incubation time, fetal bovine serum, and the resealing time on the Pt uptake. From Fig. 1 we can see that the intracellular Pt mass was linearly dependent on the extracellular cisplatin concentration in control as well as in the electroporated cells. Thus, we decided to perform all subsequent experiments with 100 μM extracellular cisplatin and scaled our results to any concentration in the tested range. In Fig. 2 we can see that 5 min after pulse delivery we reach a plateau in the intracellular Pt mass. We thus decided to perform all subsequent experiments with 10 min incubation time after electroporation. Next, we tested whether the presence of serum in the electroporation medium affects cellular uptake of Pt (Fig. 3). There was no statistical difference between the uptake with or without serum. In Fig. 4 we can see how the membrane resealed after pulse application. When describing the data with a first-order dynamics (Eq. (2)), we determined that the resealing time constant was 2.29 min. 10 min after pulse delivery was cell membrane resealed which corroborates results shown in Fig. 2.

In Fig. 5 intracellular Pt mass is shown as a function of pulse number and electric field intensity. We can see that the highest uptake was achieved with eight pulses of 1.2 kV/cm (35 ng of Pt per sample). With higher pulse number or higher electric field, the intracellular Pt mass decreased, presumably due to increased cell death, *i.e.*, reduced cell number in the sample. To explore hypothesis of cell death contribution, we also performed experiments evaluating cell death. Results are shown in Fig. 6 - in Fig. 6a is the short-term cell death measured by flow cytometry one hour after the treatment and in Fig. 6b is the metabolic activity measured by MTS assay 24 h after the treatment. We can see that the results obtained with both assays correlate well. Survival starts to decrease at electric fields above 0.6 kV/cm for any pulse number tested. With 1, 4 or 8 pulses even at the highest electric fields, the survival was not yet affected. For calculating the permeability coefficients, we have to take into account cell death and correct the

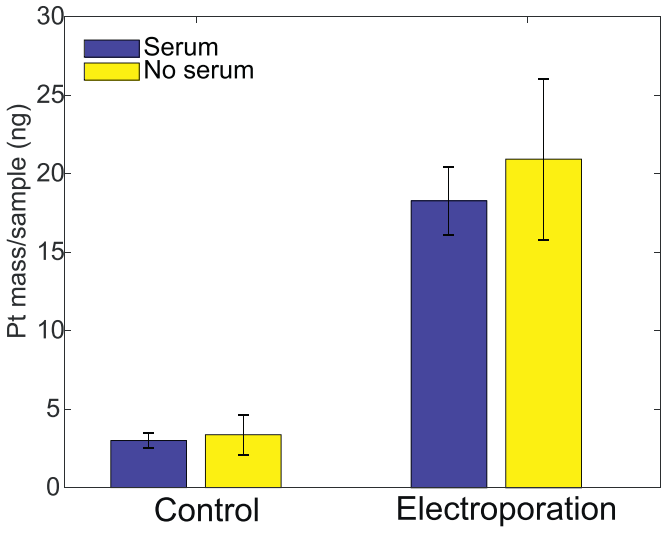

Fig. 3. Effect of the presence of serum in the electroporation medium on intracellular Pt mass (mean ± standard deviation). There was no statistical difference in pulsed and control cells when serum was or was not present. Each data point was repeated 3–5 times.

permeability coefficient.

Due to increased cell membrane permeability, different molecules and ions can enter the cell in different concentrations, depending on their size, molecular weight and charge. Small molecules (several hundred Da – *e.g.*, propidium iodide, lucifer yellow, cisplatin, yo-pro-1®) were shown to enter cells in 90–100% of their extracellular concentration [68]. In our experiments, we calculated intracellular cisplatin concentration in comparison to extracellular cisplatin concentration (Fig. 7). We reached 80% of the extracellular concentration with eight pulses of 1.2 kV/cm (Fig. 7a). Lower cell membrane permeability or cell death decreased this percentage in case of other pulse parameters. We took cell death into account by normalizing the intracellular concentration to the survival as determined by flow

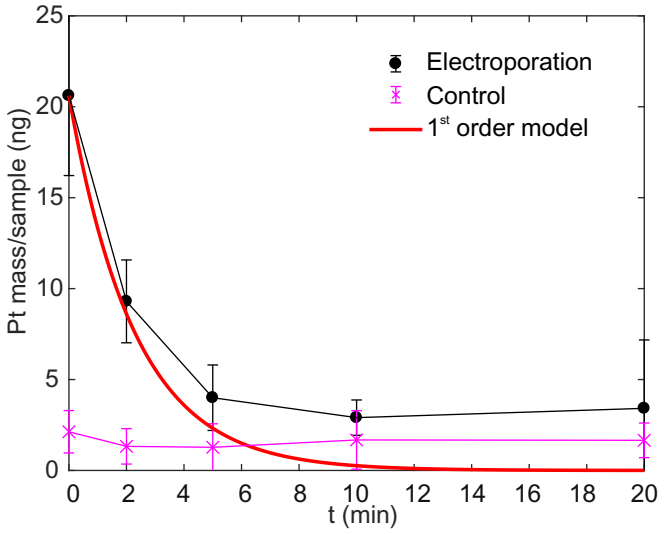

Fig. 4. Membrane resealing after 8 × 100 μs pulses of 1 kV/cm were delivered at repetition frequency 1 Hz and 100 μM cisplatin (mean ± standard deviation). Membrane resealed with a first-order dynamics with a time constant 2.29 min which is shown in red. Each data point was repeated 4–6 times. 2 and 5 min data point was statistically significantly different between electroporated and corresponding control samples ($P \leq 0.001$ for 2 min and $P = 0.045$ for 5 min). There was also a statistical difference between 2 min and 5 min electroporated samples ($P = 0.002$). All other comparisons were not significant. (For interpretation of the references to colour in this figure legend, the reader is referred to the web version of this article.)

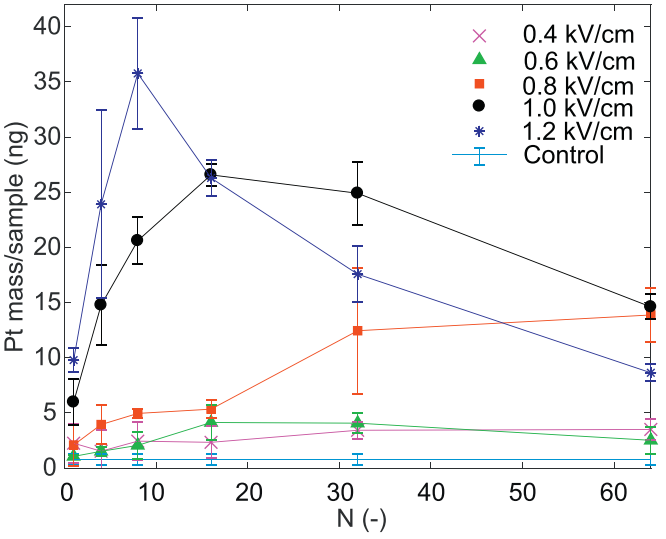

Fig. 5. Effect of a number of pulses and the electric field on the intracellular Pt mass. 8 × 100 μs pulses were delivered at repetition frequency 1 Hz and 100 μM extracellular cisplatin (mean ± standard deviation). Each data point was repeated 3–5 times. Data points were compared to the control. Comparison was not significant for 0.4 kV/cm and 1, 4 or 32 pulses; for 0.6 kV/cm and 1, 4, 8 or 64 pulses, for 0.8 kV/cm and 1 or 4 pulses. All other data points were statistically significant ($P \leq 0.05$).

cytometry (Fig. 6a) and obtained graph in Fig. 7b. There we can see that we obtain uptake higher than 100% and is increasing with increasing electric field and pulse number.

3.2. In vivo experiments

We measured the intra- and extracellular Pt mass and by taking into account the size of cells and their volume fraction also calculated the intracellular and extracellular cisplatin concentration. The concentration is just an approximation since the concentration in the tissue/tumor is most likely heterogeneous. Results are shown in Table 2.

3.3. Modeling

By using the dual-porosity model, we calculated *in vitro* permeability coefficient. We also took into account that the permeability coefficient is time dependent due to cell membrane resealing. We assumed that during resealing, the permeability of the plasma membrane decreases exponentially with time, which has been confirmed experimentally and by modeling [64, 69, 70]. Thus, the permeability coefficient also decreases exponentially with time. The resealing coefficient was obtained by fitting Eq. (2) to results, shown in Fig. 4 and optimizing the τ to obtain the highest R^2 value of the model. In Fig. 8a we can see the permeability coefficient P_0 at $t = 0$ s, *i.e.*, when electric pulses were applied, and the cell membrane was fully permeabilized and in Fig. 8b, how the permeability coefficient changed with time $P(t)$.

For the *in vivo* conditions, we modeled transport in a tumor modeled by a sphere consisting of intra- (tumor cells) and extracellular (interstitial fraction) space. In each compartment, the transport was described by the dual-porosity model. We determined the optimal diffusion coefficient to be 2.1×10^{-6} cm^2/s and the optimal transformation coefficient to be 0.3. We obtained temporal and spatial dynamics of Pt uptake in the intra- and extracellular space. To compare results of the simulation with experimental results [63], we simulated the transport one hour after pulse delivery. In the model, the Pt mass achieved plateau sooner since cell membrane resealed in 10 min (Fig. 4) but we simulated one hour more to be able to compare the simulation results with the experimental results. Results are shown in Table 3.

The concentration of Pt in a tumor one hour after electroporation as calculated by the model was heterogeneous with higher concentration in the center of a tumor and gradually decreasing to the rim of a tumor, where concentration was 0 mM (Fig. 9). Therefore, we compared the mass of Pt which was calculated as an integral over the corresponding volume fraction to the measured Pt mass in the *in vivo* experiments.

4. Discussion

Our aim was to determine whether it is possible to model the transport of chemotherapeutics in electrochemotherapy of tumors *in vivo* based on experiments performed *in vitro*. On cell suspension, experiments are easier to perform, there are no ethical issues, and a large spectrum of parameters can be explored. We could thus perform experiments *in vitro* and explore a large parameter space of electric pulses. We then connected our results with the readily available *in vivo* results and determined that a connection *in vitro – in vivo* was possible. Our study thus nevertheless requires more experiments to determine whether the connection *in vitro – in vivo* could also be obtained in other tumor types and with bleomycin.

The long-term goal of our work is to include a model of transport in treatment planning of electrochemotherapy. In treatment planning of electrochemotherapy, a critical experimentally determined electric field of permeabilization [71, 72] or statistical models [62, 73, 74] are used to determine which area will be permeabilized/affected and which not. Permeabilization alone, however, does not guarantee treatment efficacy [10]. For successful electrochemotherapy, a sufficient amount of chemotherapeutics has to enter tumor cells and bind to DNA (the main target of cisplatin) or target other molecules in the cell to prevent future cell division and cause cell death. Current treatment plans of electrochemotherapy lack a model of transport and drug uptake in a tumor and the cells. A number of internalized bleomycin molecules has been correlated with the biological effect and established that a few thousand bleomycin molecules cause mitotic death while several million cause cell death similar to apoptosis [39, 75]. A similar analysis should also be done in future for cisplatin.

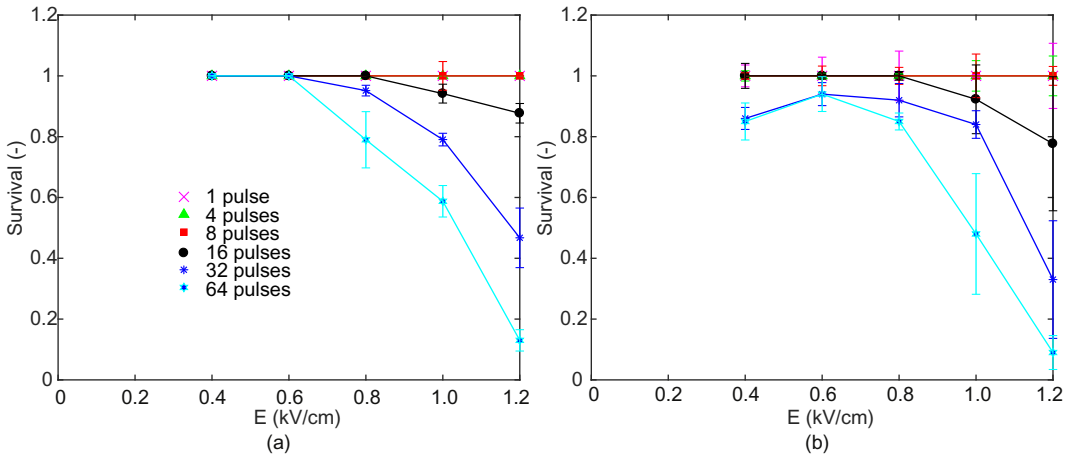

Fig. 6. Decrease in cell survival due to irreversible electroporation. (a) Survival determined by flow cytometry, one hour after electroporation and (b) by the MTS survival assay, 24 h after electroporation (mean ± standard deviation). The legend is valid for both figures. Each data point was repeated 3–6 times. In (a) the statistically significant points with respect to the control were 0.8 kV/cm and 32 or 64 pulses, 1 kV/cm at 8, 16, 32 or 64 pulses and 1.2 kV/cm at 16, 32 or 64 pulses ($P \leq 0.03$). In (b) the statistically significant points with respect to the control were 0.4 kV/cm at 8, 32 and 64 pulses, 0.8 kV/cm at 64 pulses, 1 kV/cm at 1, 32 or 64 pulses, 1.2 kV/cm at 8, 32 and 64 pulses ($P \leq 0.03$).

In our paper, we showed that it is possible to connect the *in vitro* experiments with the *in vivo* experiments. By using the dual-porosity model, we accurately calculated the Pt mass in the intra- and extracellular tumor space. Our model could eventually be used to predict treatment efficacy from a number of molecules delivered to cells as a function of the electric field in the tissue.

4.1. Experimental part

In vitro, we used mouse melanoma B16-F1 cells and *in vivo*, tumor from mouse melanoma B16-F10 cells. B16-F1 and B16-F10 cells vary only in their metastatic potential [76]. *In vitro*, increased uptake of molecules after electroporation is relatively easy to determine using fluorescent dyes and techniques like fluorescent microscopy, flow cytometry, spectrofluorometry [77]. *In vivo*, the increased uptake of molecules after electroporation is challenging to assess. ^{57}Co-bleomycin [78], ^{111}In-bleomycin [79], ^{99m}Tc-DTPA [80], ^{51}Cr-EDTA [81], gadolinium [82], lucifer yellow [83] and cisplatin [22, 23, 30, 84–88] were used previously. Cisplatin is a Pt-based chemotherapeutic what allows to calculate the concentration of cisplatin by measuring Pt mass in a

Table 2
Intra- and extracellular Pt mass and the corresponding cisplatin concentration, based on the measured volume of each tumor 2 min after injection of cisplatin (initial conditions, when electric pulses are applied, $t = 0$) and at $t = 60$ min after the therapy (cisplatin + electroporation, *i.e.*, electrochemotherapy). From the results at 60 min we subtracted the Pt in the control samples (without electroporation) to focus only on the increased uptake of cisplatin after electroporation. The intracellular Pt masses at t = 0 min and t = 60 min were statistically different ($P < .02$), *i.e.*, the intracellular Pt mass was higher after the treatment than before. The extracellular Pt mass before and after the treatment was not statistically different.

	t = 0 min (mean ± st. dev.).	t = 60 min [63] (mean ± st. dev.)
Intracellular Pt mass	17 ng ± 12 ng	67 ng ± 18 ng
Extracellular Pt mass	6431 ng ± 4681 ng	666 ng ± 104 ng
Intracellular cisplatin concentration	7 μM ± 5.5 μM	25 μM ± 10 μM
Extracellular cisplatin concentration	1600 μM ± 1200 μM	144 μM ± 110 μM

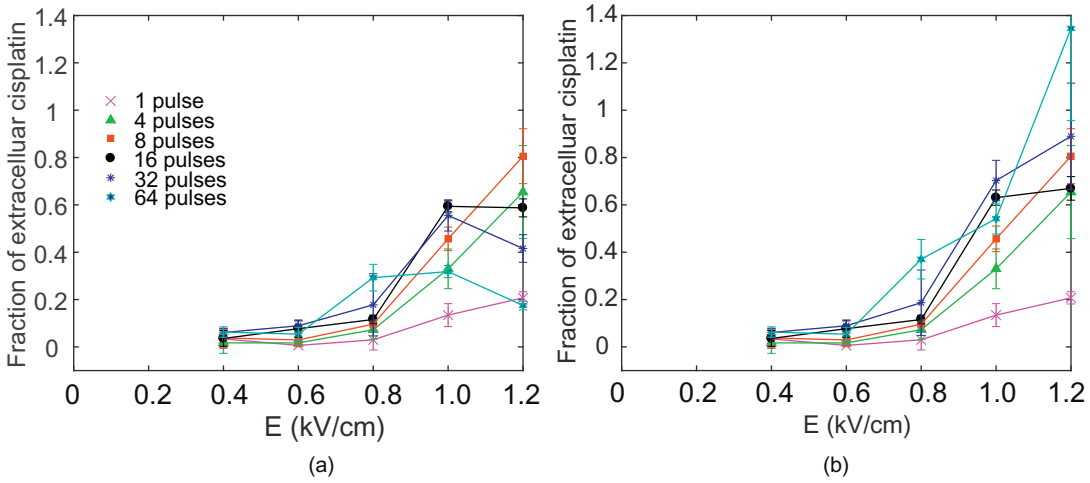

Fig. 7. The fraction of the extracellular Pt concentration, present in the intracellular compartment (mean ± standard deviation). a) Cell death was not taken into account, and the intracellular Pt concentration was almost 80% of the extracellular cisplatin concentration. b) Results of the uptake were corrected for cell death as determined by flow cytometry one hour after the treatment. The maximal value of the intracellular Pt concentration was almost 140% of the extracellular cisplatin concentration. The legend is valid for both figures.

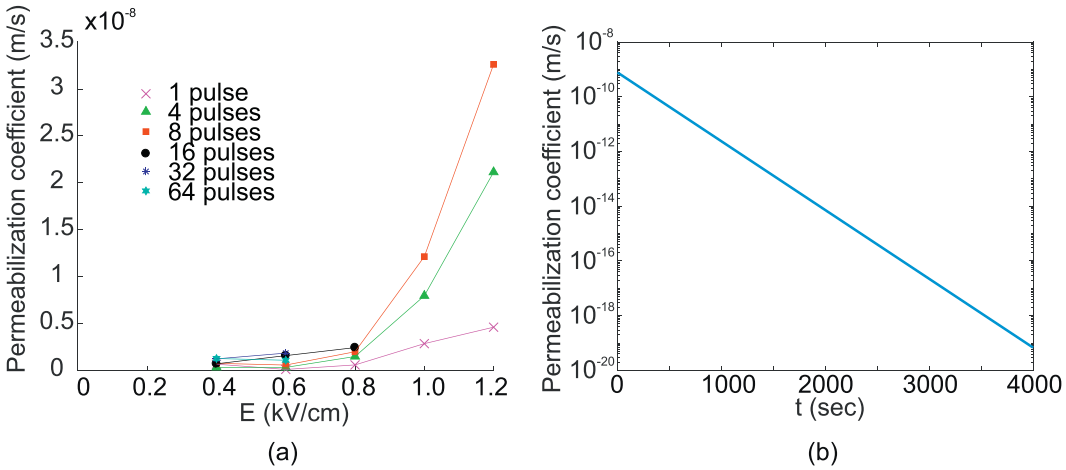

Fig. 8. The permeability coefficient determined by the dual-porosity model for conditions, where survival was 100%. a) Permeability coefficient at t = 0, *i.e.*, just after exposure to electric pulses. b) Permeability coefficient as a function of time when 8 × 100 μs pulses were delivered at 0.4 kV/cm and 1 Hz repetition frequency on a semi-logarithmic scale. The permeability coefficient on (b) was used in the *in vivo* model.

Table 3
Experimentally determined and modeled mass of Pt in the intracellular and extracellular space of a tumor 1 h after the treatment with electrochemotherapy [63].

	Experiments [63]	Model
Intracellular Pt mass	67 ng	65 ng
Extracellular Pt mass	666 ng	664 ng

known volume. The mass of Pt can be measured precisely even for very low amounts by inductively coupled plasma mass spectrometry. As Pt mass is easily determined *in vitro* as well as *in vivo*, we used cisplatin in our study. Another possibility for Pt detection is attaching a contrasting agent as a ligand to the Pt.

Before exploring the parameter space by changing the number of applied electric pulses and electric field, we tested 1) at what extracellular cisplatin concentration we should perform the experiments, 2) if fetal bovine serum can be present in the medium, 3) how long should we incubate cells after pulse delivery and 4) what was the effect of membrane resealing on intracellular Pt mass. 1) We determined that with increasing extracellular cisplatin concentration, also intracellular Pt mass increased. The dependency was linear which indicates that the increased uptake of molecules after electroporation was mostly diffusive and not electrophoretic or endocytic which is in accordance with an already published study [89]. We decided to perform experiments at 100 μM and because of the linear dependency, results could be scaled to any concentration in the tested range. 100 μM concentration was used because it is in a similar range as used in other *in vitro* studies [24, 90–92] and higher cisplatin concentration caused higher intracellular Pt mass which enabled to more accurately distinguish between intracellular masses at similar pulse parameters. 2) Fetal bovine serum added to the growth medium consists mostly of proteins. Cisplatin unspecifically binds to proteins [61] and also to collagen [93] which represents 5–10% of the matrix. The time dynamics of cisplatin binding to proteins is in a range of hours [61, 94, 95]. Cisplatin, bound to proteins, is biologically inactive [96]. Our results *in vitro* show that binding of cisplatin to proteins in the fetal bovine serum in the first 10 min was negligible (Fig. 3). Because cisplatin was observed to bind to proteins in a time-range of hours-days, we did not include cisplatin binding in the tumor model. 3) When we tested the influence of incubation time after electric pulse application, we determined that a plateau is reached after 5 min (Fig. 2). Thus, we decided to wait in all our experiments for 10 min after pulse application when the uptake due to electroporation ended. The reason for reaching a plateau could be that the increased uptake of molecules after electroporation is much faster than the passive diffusion or active mechanisms, which exist in

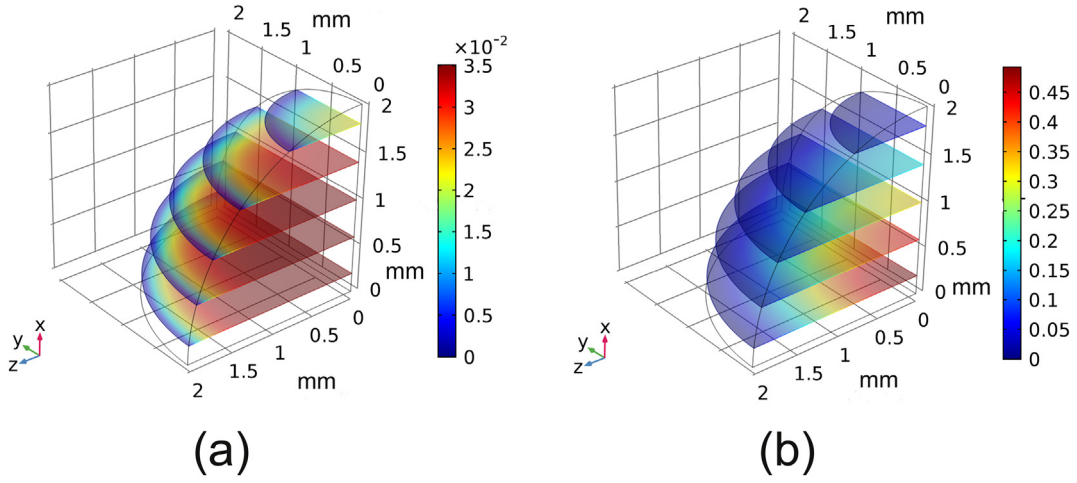

Fig. 9. Modeled spatial dependency of Pt concentration 1 h after pulse delivery in mol/m^3. (a) Intra- and (b) extracellular Pt concentration. Spatial distribution is heterogeneous in both cases. The spatial coordinate is given in mm. Please, note different scales of the concentration on a) and b).

the cells. Namely, it was shown that without electroporation, intracellular cisplatin concentration increases in a time-range of hours, *in vitro* as well as *in vivo* [32, 97] The additional mechanisms could contribute to a higher transport and increase in the uptake on a longer timescale. To focus only on the modeling uptake due to electroporation, we subtracted the mass of the Pt in the control samples from the mass of Pt in treated samples when calculating the permeability coefficient and comparing the results of our model with the experiments.

Electrochemotherapy is usually performed with 8 × 100 μs pulses. However, we wanted our model to be valid in a larger parameter space, which would enable its use also with other pulse parameters. Thus, we applied *in vitro* 1 to 64 pulses. With increasing pulse number and electric field, the intracellular Pt mass increased with a peak at eight 100 μs pulses of 1.2 kV/cm (Fig. 5). We calculated the volume of all cells ($\approx 2\ mm^3$) in a sample and using the measured Pt mass in the cells calculated the intracellular Pt concentration. We determined that the intracellular Pt concentration is up to 80% of the extracellular cisplatin concentration (Fig. 7a). The high percentage is in agreement with the mass of the cisplatin (300 g/mol) [68]. With some parameters of electric pulses, we were already irreversibly electroporating cells (Fig. 6) which also affected the determination. The uptake was decreased as can be observed in the shape of the curves in Fig. 5, *i.e.*, we reach maximum at lower pulse number (eight pulses at 1.2 kV/cm or 16 pulses at 1.0 kV/cm) and then with increasing pulse number the uptake decreases. We thus normalized the percentage of intracellular cisplatin concentration to survival and obtained values higher than 100% (Fig. 7b) which indicates that either 1) cisplatin binds to DNA and concentration gradient increases, and/or 2) cell death was not the only reason for decreased uptake, and/or 3) some other cell death assay would be more suitable, and/or 4) active mechanisms additionally transport cisplatin into cells. We determined that eight pulses are the optimal number to be delivered which is consistent with the standard electrochemotherapy protocol [19, 21]. In our *in vivo* model, we used the permeability coefficient when cell survival was 100%.

In the *in vivo* experiments, we injected 26 μg of Pt by intratumoral injection of 80 μl of cisplatin in 35 mm^3 tumors. The volume of injection was twice the volume of a tumor because we reused the data from [63] to follow the 3Rs of the animal experiments [98]. Most of the injected Pt was not measured. When a tumor was excised 2 min after cisplatin injection, we determined that 27% of the injected Pt was still present in a tumor and the serum. A part of cisplatin was lost due to lower tumor volume than injection volume and due to washout of cisplatin from the tumor. When a tumor was excised after 1 h, we determined that in a tumor and serum there was 2% of the injected Pt in the control samples (cisplatin injection, no electroporation) and 7% in the treated (cisplatin injection and electroporation) samples. Thus, *in vivo,* the majority of cisplatin was unaccounted for. Part of cisplatin was lost due to the used methodology (when the tumor was mechanically disintegrated and during blood collection) and part of cisplatin could accumulate in different organs and cause unwanted side effects [99].

4.2. Modeling part

Our model is based on a hypothesis that cell membrane permeability *in vitro* and *in vivo* is similar when cells are exposed to the same electric field and pulse parameters. However, the transport *in vivo* is decreased in comparison to the transport *in vitro* due to the hindered transport of molecules in the *in vivo* environment due to the cell matrix, lower diffusion coefficient of molecules in the interstitial space and close cell contacts. The transformation of the transport model from the *in vitro* to the *in vivo* environment is challenging. We can use the *in vitro* permeability coefficient in the *in vivo* model, as long as we take into account the geometric characteristics of tissue (cell volume fraction, cell matrix volume fraction, cell size). We took the characteristics into account by decreasing the transport by the transformation coefficient. In our model, we assume that the transformation coefficient is a function of tissue morphology and decreases with increasing cell volume fraction and matrix volume fraction. It remains to be tested if the transformation coefficient can be used over several values of parameters of electric pulses and cisplatin concentration and if transformation coefficient is a function of experimental conditions (*e.g.*, tumor cell volume fraction) [66].

Our initial conditions of the *in vivo* model were homogeneously distributed 1.6 mM cisplatin in the tumor interstitial fraction. Initial cisplatin concentration was determined from experiments by excising tumors 2 min after cisplatin injection when usually electric pulses were applied. According to our calculations, the initial cisplatin concentration in a tumor (1.6 mM) was similar to the concentration injected (1.65 mM), which means that by injecting cisplatin we washed out the interstitial fluid and replaced it with cisplatin. Thus, part of cisplatin volume was lost due to washout from the tumor, but the remaining cisplatin was not diluted in the interstitial fraction, and it remained at (almost) initial concentration. Initial cisplatin distribution was determined from the literature [23, 100]. Solutes are washed out relatively quickly from small tumors and with some delay from larger tumors [100]. In [23] it was determined that electrochemotherapy treatment was most efficient when electric pulses were delivered 0–5 min after intratumoral cisplatin injection. This time scale indicates that in the first 5 min after intratumoral injection the cisplatin distribution in a tumor is approximately homogeneous and not yet washed out of a tumor. 0–5 min was a similar time range as used in our experiments (2 min) implying that approximating the initial cisplatin distribution in the model as homogeneous is justified. In future, for experimental determination of initial cisplatin distribution, a technique like imaging mass cytometry could be used [93]. At 60 min after the treatment, the cisplatin concentration was the highest in the center of the tumor, which corresponds to previously published data – in [83] a fluorescent dye was injected, and in the tissue sections it can be seen that the dye reached its highest concentration in the center of the sample.

The volume fraction of cells in a tumor was calculated by the method presented in [67] - the surface fraction of cells determined on a slice is a good approximation of volume fraction. We used experimental data [66] where the volume fraction of cells and cell matrix and cell size in B16-F1 mouse melanoma tumors were assessed. We calculated cell volume fraction of 37% in tumors. Since a tumor has a high cellular fraction in comparison to our *in vitro* results, we took that into account. The high volume fraction of cells decreases the induced transmembrane voltage due to electric field shielding [41, 101]. Considering the calculations in [102, 103] we can determine that the induced transmembrane voltage in cells *in vivo* is 76–88% of the one induced on a single spherical cell. The average radius of cells *in vivo* was determined to be 6.25 μm [66] which is less than the average *in vitro* radius of 8.1 ± 1.1 μm [65] which means that according to Schwann equation, the induced transmembrane on the cells *in vivo* is 77% of the *in vitro* induced transmembrane voltage. We thus have to take into account the decrease in induced transmembrane voltage due to cell proximity and smaller cells *in vivo*. Considering this, the induced transmembrane voltage *in vivo* is approximately 60% of the one induced on cells *in vitro* at the same external electric field. The voltage-to-distance ratio delivered to a tumor by parallel plate electrodes was 1.3 kV/cm. It was numerically determined that the electric field in a tumor was inhomogeneous [38], and in the center of a tumor, it was 0.6 kV/cm. Taking into account the lower induced transmembrane voltage on the cells *in vivo*, the conditions *in vivo* correspond to when 0.34–0.4 kV/cm is delivered *in vitro*. Thus, the *in vitro* permeability coefficient when eight 100 μs, 0.4 kV/cm at 1 Hz were applied *in vitro* was used in the tumor model. We also took into account cell resealing after pulse application and the decrease in cell permeability coefficient. From the *in vitro* results, we determined the time constant of resealing was 2.29 min which is in agreement with the *in vivo* data (Fig. 2 in [23]). When eight pulses at 0.4 kV/cm were delivered the survival was still 100% (Fig. 6),

and there was no need for permeability coefficient correction. The calculated value of 0.4 kV/cm is also in agreement with the literature where 0.4 kV/cm is usually assumed to be a threshold of electroporation for a tumor [83, 104].

In tumors, the transport differs from normal tissues, as tumors have an abnormal vasculature and increased interstitial pressure which facilitates cisplatin washout [105, 106]. In the interstitial space, two mechanisms of transport are present – diffusion and convection. The diffusion in tissues is lower than in water as tissue structures obstruct the transport. In the literature, values of diffusion coefficient for cisplatin or similar molecules are reported in the range of $0.1–0.7 \times 10^{-6}$ cm^2/s [107–109] which is less than the value we determined in our model (2.1×10^{-6} cm^2/s). Electric pulses cause a vascular lock which is present in the time range of hours, although blood flow is to some extent restored in first 15 min [44]. It is possible that the diffusion constant in our study is higher because a part of the transport out of a tumor was due to convection, while we limited our analysis to diffusion. However, convection introduces a new unknown parameter (velocity) in the model, and here we decided to model the transport as only diffusive. Also, vasoconstriction due to electric pulses decreases convective transport from the tumor. In future, the convective transport could be included, but experimental data are needed first.

All models include simplifications. In our model, the following simplifications were made and should be considered. 1) The tumor was modeled as a sphere, and its physiology was considered to be homogeneous throughout the tumor. Also, the initial intracellular concentration and the electric field in the tumor were considered to be homogeneous. 2) *In vivo*, one combination of parameters of electric pulses was tested (1.3 kV/cm voltage over the distance between the electrodes, 8 × 100 μs pulses applied at 1 Hz repetition frequency). 3) We modeled the uptake of one chemotherapeutic, *i.e.*, cisplatin. 4) We modeled one tumor type, *i.e.*, melanoma. 5) We modeled one route of administration, *i.e.*, intratumoral.

The justifications for the simplifications are the following. 1) We modeled the tumor as a symmetrical sphere, thus decreasing the complexity of the model and time of calculation, which was justifiable because mouse melanomas used in our experiments were spherical due to a localized injection during inoculation. Further, its necrotic areas were distributed throughout the whole tumor (a photo and the histology of the tumor are available in the Supplemental File). However, our model also supports other geometries; the only adaptations required would be those of the geometry and the mesh. In reality, the electric field in the tumor is inhomogeneous [38, 83] which could be later included as spatially dependent permeability coefficient. We approximated initial cisplatin distribution in the tumor as homogeneous and the cisplatin concentration at the external border of a tumor to be 0 mM, although in reality there is a smooth transition in the concentration between intra- and extratumoral cisplatin. However, the initial spatial cisplatin distribution after intratumoral delivery was to the best of our knowledge not yet determined. The size of the cells *in vitro* is statistically distributed [57] which could in future be included in the calculation of the permeabilization coefficient. 2) We have applied electric pulses *in vivo* at only one pulse number, duration, and electric field. Thus our model is strictly speaking only valid at 1.3 kV/cm voltage over the distance, 8 × 100 μs pulses between the electrodes, which nevertheless is a standard treatment parameter in electrochemotherapy. 3) The model was tested with cisplatin, which is one of the two drugs used in electrochemotherapy treatments and its intracellular mass after electroporation has been determined under different experimental conditions [22, 23, 30, 63, 84–87]. Another molecule used in electrochemotherapy is bleomycin [18] whose concentration can be determined by liquid chromatography coupled to high-resolution mass spectrometry, as only recently demonstrated [110, 111]. Similarly, any other molecule whose intracellular concentration we can determine, could be used in the model. 4) Our model was tested on only one type of a tumor, more *in vivo* experiments are needed, preferably with different tumor types. Our current hypothesis is that different tumor types will affect the diffusion coefficient of cisplatin and the transformation coefficient in the interstitial tumor fraction depending on the volume fraction of cells in the tumor, both decreasing with the increased volume fraction of cells in the tumor. Also, different sizes and volume fractions of cells in different tumors affect the induced transmembrane voltage [102, 103]. Permeability coefficient for different tumor types should be calculated from the experiments on corresponding cell types *in vitro* as different cells exhibit different sensitivity to electric pulses [112]. 5) We modeled intratumoral cisplatin delivery as suggested in the Standard Operating Procedures of electrochemotherapy [19, 21]. However, for our model to be useful for intravenous (i.v.) drug delivery, additional steps would have to be performed to determine the initial spatial drug concentration in the tumor. In the i.v. delivery, the drug has to overcome several obstacles before entering the tumor – it has to extravasate from the blood vessels, reach the tumor, overcome the increased interstitial pressure and distribute throughout the interstitial tumor fraction [48, 105]. Modeling different delivery routes is a large field of ongoing research [48]. Different delivery routes could be coupled to our model and calculated separately as a 'pre-model'.

In future, upgrades to our model are possible. We could include kinetics of the binding of cisplatin to the DNA and resulting cell death as was previously described at a cell level [113–116]. With our model, we could predict not only the intracellular cisplatin concentration but also cell death as a function of the electric field in the tissue and injected cisplatin dose. For this, however, we would need to additionally determine the number of molecules in the cell to achieve cell death.

To conclude, we designed our feasibility study as a test whether *in vivo* drug transport could be calculated from results of the *in vitro* experiments. Since we obtained positive results, more experiments are now warranted to validate our model in a wider range of experimental conditions with respect to tumor type, choice of the drug and administration route. We aim to decrease the number of *in vivo* electrochemotherapy experiments, as *in vitro* experiments should give adequate results without the need for extensive parameter testing *in vivo*.

5. Conclusions

With electrochemotherapy, we can effectively treat tumors with a combination of delivering chemotherapeutics and electric pulses. To predict the treatment outcome or optimize the position of the electrodes, we first calculate the electric field distribution. We use the critical electric field for reversible electroporation to determine reversibly electroporated area, *i.e.*, the area where electrochemotherapy would be efficient. In this study, we introduced a model of drug transport that described the transport of cisplatin after intratumoral injection and application of electric pulses in subcutaneous mouse melanoma tumor. We modeled the transport of chemotherapeutic between several compartments – tumor cells, interstitial tumor fraction, and peritumoral environment using the dual-porosity model. We described the uptake of cisplatin *in vivo* by using the permeability coefficient from *in vitro* experiments. By optimizing the parameters of the treatment *in vitro*, a large spectrum of parameters could be easily tested, and a number of experiments on animals could be reduced. We demonstrated that it is possible to connect the experiments at the cell level (*in vitro)* to the tissue level (*in vivo)*. By including the calculation of the drug transport into treatment planning of electrochemotherapy, the precision of the outcome could be increased. More experimental work is however needed to validate our model using different tumor types, chemotherapeutics, and their delivery routes.

Acknowledgments

This work was supported by the Slovenian Research Agency (ARRS) [research core funding No. P2-0249, P3-0003, and IP-0510, and

funding for Junior Researchers to JDČ and KU]. The research was conducted within the scope of the electroporation in Biology and Medicine (EBAM) European Associated Laboratory (LEA). JDČ would like to thank D. Hodžić and L. Vukanović for their help in the cell culture laboratory, Dr. S. Mahnič-Kalamiza for discussions on the dual-porosity model, and Dr. T. Kotnik for proofreading the paper.

Declarations of interest

None.

Appendix A. Supplementary data

Supplementary data to this article can be found online at https://doi.org/10.1016/j.jconrel.2018.07.021.

References

[1] T. Kotnik, P. Kramar, G. Pucihar, D. Miklavčič, M. Tarek, Cell membrane electroporation- part 1: the phenomenon, IEEE Electr. Insul. Mag. 28 (2012) 14–23, https://doi.org/10.1109/MEI.2012.6268438.
[2] T.Y. Tsong, Electroporation of cell membranes, Biophys. J. 60 (1991) 297–306, https://doi.org/10.1016/S0006-3495(91)82054-9.
[3] J.C. Weaver, Electroporation of cells and tissues, IEEE Trans. Plasma Sci. 28 (2000) 24–33, https://doi.org/10.1109/27.842820.
[4] L. Rems, D. Miklavčič, Tutorial: electroporation of cells in complex materials and tissue, J. Appl. Phys. 119 (2016) 201101, , https://doi.org/10.1063/1.4949264.
[5] T. Kotnik, W. Frey, M. Sack, S. Haberl Meglič, M. Peterka, D. Miklavčič, Electroporation-based applications in biotechnology, Trends Biotechnol. (2015), https://doi.org/10.1016/j.tibtech.2015.06.002.
[6] S. Mahnič-Kalamiza, E. Vorobiev, D. Miklavčič, Electroporation in food processing and biorefinery, J. Membr. Biol. 247 (2014) 1279–1304.
[7] J. Blahovec, E. Vorobiev, N. Lebovka, Pulsed electric fields pretreatments for the cooking of foods, Food Eng. Rev. 9 (2017) 226–236, https://doi.org/10.1007/s12393-017-9170-x.
[8] M.L. Yarmush, A. Golberg, G. Serša, T. Kotnik, D. Miklavčič, Electroporation-based Technologies for Medicine: principles, applications, and challenges, Annu. Rev. Biomed. Eng. 16 (2014) 295–320, https://doi.org/10.1146/annurev-bioeng-071813-104622.
[9] D. Miklavčič, R.V. Davalos, Electrochemotherapy (ECT) and irreversible electroporation (IRE) -advanced techniques for treating deep-seated tumors based on electroporation, Biomed. Eng. Online 14 (2015) I1, https://doi.org/10.1186/1475-925X-14-S3-I1.
[10] D. Miklavčič, B. Mali, B. Kos, R. Heller, G. Serša, Electrochemotherapy: from the drawing board into medical practice, Biomed. Eng. Online 13 (2014) 29, https://doi.org/10.1186/1475-925X-13-29.
[11] D.E. Spratt, E.A. Gordon Spratt, S. Wu, A. Derosa, N.Y. Lee, M.E. Lacouture, C.A. Barker, Efficacy of skin-directed therapy for cutaneous metastases from advanced cancer: a meta-analysis, J. Clin. Oncol. Off. J. Am. Soc. Clin. Oncol. 32 (2014) 3144–3155, https://doi.org/10.1200/JCO.2014.55.4634.
[12] R. Heller, L.C. Heller, Gene electrotransfer clinical trials, Adv. Genet. (2015) 235–262 http://linkinghub.elsevier.com/retrieve/pii/S0065266014000078 , Accessed date: 26 January 2016(Elsevier).
[13] S. Vasan, A. Hurley, S.J. Schlesinger, D. Hannaman, D.F. Gardiner, D.P. Dugin, M. Boente-Carrera, R. Vittorino, M. Caskey, J. Andersen, Y. Huang, J.H. Cox, T. Tarragona-Fiol, D.K. Gill, H. Cheeseman, L. Clark, L. Dally, C. Smith, C. Schmidt, H.H. Park, J.T. Kopycinski, J. Gilmour, P. Fast, R. Bernard, D.D. Ho, In vivo electroporation enhances the immunogenicity of an HIV-1 DNA vaccine candidate in healthy volunteers, PLoS ONE 6 (2011) e19252, , https://doi.org/10.1371/journal.pone.0019252.
[14] C. Jiang, R.V. Davalos, J.C. Bischof, A review of basic to clinical studies of irreversible electroporation therapy, IEEE Trans. Biomed. Eng. 62 (2015) 4–20, https://doi.org/10.1109/TBME.2014.2367543.
[15] R.V. Davalos, L.M. Mir, B. Rubinsky, Tissue ablation with irreversible electroporation, Ann. Biomed. Eng. 33 (2005) 223–231, https://doi.org/10.1007/s10439-005-8981-8.
[16] B. Zorec, V. Préat, D. Miklavčič, N. Pavšelj, Active enhancement methods for intra- and transdermal drug delivery: a review, Zdr. Vestn. 82 (2013) 339–356.
[17] N. Dujardin, E. Staes, Y. Kalia, P. Clarys, R. Guy, V. Préat, In vivo assessment of skin electroporation using square wave pulses, J. Control. Release 79 (2002) 219–227.
[18] M. Marty, G. Serša, J.R. Garbay, J. Gehl, C.G. Collins, M. Snoj, V. Billard, P.F. Geertsen, J.O. Larkin, D. Miklavčič, I. Pavlović, S.M. Paulin-Košir, M. Čemažar, N. Morsli, D.M. Soden, Z. Rudolf, C. Robert, G.C. O'Sullivan, L.M. Mir, Electrochemotherapy – an easy, highly effective and safe treatment of cutaneous and subcutaneous metastases: results of ESOPE (European standard operating procedures of Electrochemotherapy) study, Eur. J. Cancer Suppl. 4 (2006) 3–13, https://doi.org/10.1016/j.ejcsup.2006.08.002.
[19] L.M. Mir, J. Gehl, G. Serša, C.G. Collins, J.-R. Garbay, V. Billard, P.F. Geertsen, Z. Rudolf, G.C. O'Sullivan, M. Marty, Standard operating procedures of the electrochemotherapy: instructions for the use of bleomycin or cisplatin administered either systemically or locally and electric pulses delivered by the CliniporatorTM by means of invasive or non-invasive electrodes, Eur. J. Cancer Suppl. 4 (2006) 14–25.
[20] J.-M. Escoffre, M.-P. Rols, Electrochemotherapy: progress and prospects, Curr. Pharm. Des. 18 (2012) 3406–3415.
[21] J. Gehl, G. Serša, L.W. Matthiessen, T. Muir, D. Soden, A. Occhini, P. Quaglino, P. Curatolo, L.G. Campana, C. Kunte, A.J.P. Clover, G. Bertino, V. Farricha, J. Odili, K. Dahlstrom, M. Benazzo, L.M. Mir, Updated standard operating procedures for electrochemotherapy of cutaneous tumours and skin metastases, Acta Oncol. (2018) 1–9, https://doi.org/10.1080/0284186X.2018.1454602.
[22] J.E. Melvik, E.O. Pettersen, P.B. Gordon, P.O. Seglen, Increase in cis-dichlorodiammineplatinum (II) cytotoxicity upon reversible electropermeabilization of the plasma membrane in cultured human NHIK 3025 cells, Eur. J. Cancer Clin. Oncol. 22 (1986) 1523–1530.
[23] M. Čemažar, R. Milačič, D. Miklavčič, V. Dolzan, G. Serša, Intratumoral cisplatin administration in electrochemotherapy: antitumor effectiveness, sequence dependence and platinum content, Anti-Cancer Drugs 9 (1998) 525–530, https://doi.org/10.1097/00001813-199807000-00002.
[24] G. Serša, M. Čemažar, D. Miklavčič, Antitumor effectiveness of electrochemotherapy with cis-diamminedichloroplatinum(II) in mice, Cancer Res. 55 (1995) 3450–3455.
[25] G. Serša, B. Štabuc, M. Čemažar, D. Miklavčič, Z. Rudolf, Electrochemotherapy with cisplatin: clinical experience in malignant melanoma patients, Clin. Cancer Res. Off. J. Am. Assoc. Cancer Res. 6 (2000) 863–867.
[26] G. Serša, B. Štabuc, M. Čemažar, B. Jančar, D. Miklavčič, Z. Rudolf, Electrochemotherapy with cisplatin: potentiation of local cisplatin antitumour effectiveness by application of electric pulses in cancer patients, Eur. J. Cancer 34 (1998) 1213–1218, https://doi.org/10.1016/S0959-8049(98)00025-2.
[27] S. Spreckelmeyer, C. Orvig, A. Casini, Cellular transport mechanisms of cytotoxic Metallodrugs: an overview beyond cisplatin, Molecules 19 (2014) 15584–15610, https://doi.org/10.3390/molecules191015584.
[28] D. Gately, S. Howell, Cellular accumulation of the anticancer agent cisplatin: a review, Br. J. Cancer 67 (1993) 1171–1176, https://doi.org/10.1038/bjc.1993.221.
[29] D.-W. Shen, L.M. Pouliot, M.D. Hall, M.M. Gottesman, Cisplatin resistance: a cellular self-defense mechanism resulting from multiple epigenetic and genetic changes, Pharmacol. Rev. 64 (2012) 706–721, https://doi.org/10.1124/pr.111.005637.
[30] M. Čemažar, D. Miklavčič, L. Mir, J. Belehradek, M. Bonnay, D. Fourcault, G. Serša, Electrochemotherapy of tumours resistant to cisplatin, Eur. J. Cancer 37 (2001) 1166–1172, https://doi.org/10.1016/S0959-8049(01)00091-0.
[31] A.-M. Florea, D. Büsselberg, Cisplatin as an anti-tumor drug: cellular mechanisms of activity, drug resistance and induced side effects, Cancer 3 (2011) 1351–1371, https://doi.org/10.3390/cancers3011351.
[32] A. Johnsson, C. Olsson, O. Nygren, M. Nilsson, B. Seiving, E. Cavallin-Stahl, Pharmacokinetics and tissue distribution of cisplatin in nude mice: platinum levels and cisplatin-DNA adducts, Cancer Chemother. Pharmacol. 37 (1995) 23–31, https://doi.org/10.1007/BF00685625.
[33] D. Miklavčič, G. Serša, E. Brecelj, J. Gehl, D. Soden, G. Bianchi, P. Ruggieri, C.R. Rossi, L.G. Campana, T. Jarm, Electrochemotherapy: technological advancements for efficient electroporation-based treatment of internal tumors, Med. Biol. Eng. Comput. 50 (2012) 1213–1225, https://doi.org/10.1007/s11517-012-0991-8.
[34] D. Pavliha, B. Kos, A. Županič, M. Marčan, G. Serša, D. Miklavčič, Patient-specific treatment planning of electrochemotherapy: procedure design and possible pitfalls, Bioelectrochemistry 87 (2012) 265–273.
[35] P.A. Garcia, B. Kos, J.H. Rossmeisl, D. Pavliha, D. Miklavčič, R.V. Davalos, Predictive therapeutic planning for irreversible electroporation treatment of spontaneous malignant glioma, Med. Phys. 44 (2017) 4968–4980, https://doi.org/10.1002/mp.12401.
[36] I. Edhemović, E. Brecelj, G. Gasljevič, M. Marolt Mušič, V. Gorjup, B. Mali, T. Jarm, B. Kos, D. Pavliha, B. Grčar Kuzmanov, M. Čemažar, M. Snoj, D. Miklavčič, E.M. Gadžijev, G. Serša, Intraoperative electrochemotherapy of colorectal liver metastases: Electrochemotherapy of liver metastases, J. Surg. Oncol. 110 (2014) 320–327.
[37] A. Županič, B. Kos, D. Miklavčič, Treatment planning of electroporation-based medical interventions: electrochemotherapy, gene electrotransfer and irreversible electroporation, Phys. Med. Biol. 57 (2012) 5425–5440, https://doi.org/10.1088/0031-9155/57/17/5425.
[38] D. Miklavčič, S. Čorović, G. Pucihar, N. Pavšelj, Importance of tumour coverage by sufficiently high local electric field for effective electrochemotherapy, Eur. J. Cancer Suppl. 4 (2006) 45–51, https://doi.org/10.1016/j.ejcsup.2006.08.006.
[39] O. Tounekti, G. Pron, J. Belehradek, L.M. Mir, Bleomycin, an apoptosis-mimetic drug that induces two types of cell death depending on the number of molecules internalized, Cancer Res. 53 (1993) 5462–5469.
[40] S. Mahnič-Kalamiza, D. Miklavčič, E. Vorobiev, Dual-porosity model of solute diffusion in biological tissue modified by electroporation, Biochim. Biophys. Acta Biomembr. 1838 (2014) 1950–1966, https://doi.org/10.1016/j.bbamem.2014.03.004.
[41] G. Pucihar, T. Kotnik, J. Teissié, D. Miklavčič, Electropermeabilization of dense cell suspensions, Eur. Biophys. J. 36 (2007) 172–185.
[42] P.J. Canatella, M.M. Black, D.M. Bonnichsen, C. McKenna, M.R. Prausnitz, Tissue electroporation: quantification and analysis of heterogeneous transport in multicellular environments, Biophys. J. 86 (2004) 3260–3268, https://doi.org/10.1016/S0006-3495(04)74374-X.

[43] L. Gibot, L. Wasungu, J. Teissié, M.-P. Rols, Antitumor drug delivery in multicellular spheroids by electropermeabilization, J. Control. Release 167 (2013) 138–147, https://doi.org/10.1016/j.jconrel.2013.01.021.

[44] G. Serša, T. Jarm, T. Kotnik, A. Coer, M. Podkrajsek, M. Šentjurc, D. Miklavčič, M. Kadivec, S. Kranjc, A. Secerov, M. Čemažar, Vascular disrupting action of electroporation and electrochemotherapy with bleomycin in murine sarcoma, Br. J. Cancer 98 (2008) 388–398, https://doi.org/10.1038/sj.bjc.6604168.

[45] L.T. Baxter, R.K. Jain, Transport of fluid and macromolecules in tumors. I. Role of interstitial pressure and convection, Microvasc. Res. 37 (1989) 77–104, https://doi.org/10.1016/0026-2862(89)90074-5.

[46] L.T. Baxter, R.K. Jain, Transport of fluid and macromolecules in tumors. II. Role of heterogeneous perfusion and lymphatics, Microvasc. Res. 40 (1990) 246–263, https://doi.org/10.1016/0026-2862(90)90023-K.

[47] L.T. Baxter, R.K. Jain, Transport of fluid and macromolecules in tumors: III. Role of binding and metabolism, Microvasc. Res. 41 (1991) 5–23, https://doi.org/10.1016/0026-2862(91)90003-T.

[48] A.W. El-Kareh, T.W. Secomb, Theoretical models for drug delivery to solid tumors, Crit. Rev. Biomed. Eng. 25 (1997) 503–571.

[49] P.J. Canatella, M.R. Prausnitz, Prediction and optimization of gene transfection and drug delivery by electroporation, Gene Ther. 8 (2001) 1464–1469, https://doi.org/10.1038/sj.gt.3301547.

[50] E. Neumann, K. Toensing, S. Kakorin, P. Budde, J. Frey, Mechanism of electroporative dye uptake by mouse B cells, Biophys. J. 74 (1998) 98–108, https://doi.org/10.1016/S0006-3495(98)77771-9.

[51] D. Miklavčič, L. Towhidi, Numerical study of the electroporation pulse shape effect on molecular uptake of biological cells, Radiol. Oncol. 44 (2010), https://doi.org/10.2478/v10019-010-0002-3.

[52] Y. Granot, B. Rubinsky, Mass transfer model for drug delivery in tissue cells with reversible electroporation, Int. J. Heat Mass Transf. 51 (2008) 5610–5616, https://doi.org/10.1016/j.ijheatmasstransfer.2008.04.041.

[53] J. Li, H. Lin, Numerical simulation of molecular uptake via electroporation, Bioelectrochemistry 82 (2011) 10–21, https://doi.org/10.1016/j.bioelechem.2011.04.006.

[54] S. Movahed, D. Li, Electrokinetic transport through the nanopores in cell membrane during electroporation, J. Colloid Interface Sci. 369 (2012) 442–452, https://doi.org/10.1016/j.jcis.2011.12.039.

[55] S. Movahed, D. Li, Electrokinetic transport of nanoparticles to opening of nanopores on cell membrane during electroporation, J. Nanopart. Res. 15 (2013), https://doi.org/10.1007/s11051-013-1511-y.

[56] K.C. Smith, J.C. Weaver, Transmembrane molecular transport during versus after extremely large, nanosecond electric pulses, Biochem. Biophys. Res. Commun. 412 (2011) 8–12, https://doi.org/10.1016/j.bbrc.2011.06.171.

[57] M. Puc, T. Kotnik, L.M. Mir, D. Miklavčič, Quantitative model of small molecules uptake after in vitro cell electropermeabilization, Bioelectrochemistry 60 (2003) 1–10.

[58] A. Agarwal, M. Wang, J. Olofsson, O. Orwar, S.G. Weber, Control of the release of freely diffusing molecules in single-cell electroporation, Anal. Chem. 81 (2009) 8001–8008, https://doi.org/10.1021/ac9010292.

[59] S. Mahnič-Kalamiza, D. Miklavčič, E. Vorobiev, Dual-porosity model of mass transport in electroporated biological tissue: simulations and experimental work for model validation, Innovative Food Sci. Emerg. Technol. 29 (2015) 41–54, https://doi.org/10.1016/j.ifset.2014.09.011.

[60] S. Mahnič-Kalamiza, N. Poklar Ulrih, E. Vorobiev, D. Miklavčič, A comprehensive theoretical study of thermal relations in plant tissue following electroporation, Int. J. Heat Mass Transf. 111 (2017) 150–162, https://doi.org/10.1016/j.ijheatmasstransfer.2017.03.119.

[61] A. Martinčič, M. Čemažar, G. Serša, V. Kovač, R. Milačič, J. Ščančar, A novel method for speciation of Pt in human serum incubated with cisplatin, oxaliplatin and carboplatin by conjoint liquid chromatography on monolithic disks with UV and ICP-MS detection, Talanta 116 (2013) 141–148, https://doi.org/10.1016/j.talanta.2013.05.016.

[62] J. Dermol, D. Miklavčič, Mathematical models describing Chinese hamster ovary cell death due to electroporation in vitro, J. Membr. Biol. 248 (2015) 865–881, https://doi.org/10.1007/s00232-015-9825-6.

[63] K. Uršič, Š. Kos, U. Kamenšek, M. Čemažar, J. Ščančar, S. Bucek, S. Kranjc, B. Staresinic, G. Serša, Comparable effectiveness and immunomodulatory actions of oxaliplatin and cisplatin in electrochemotherapy of murine melanoma, Bioelectrochemistry 119 (2018) 161–171, https://doi.org/10.1016/j.bioelechem.2017.09.009.

[64] J. Dermol, O.N. Pakhomova, A.G. Pakhomov, D. Miklavčič, Cell Electrosensitization exists only in certain electroporation buffers, PLoS ONE 11 (2016) e0159434, , https://doi.org/10.1371/journal.pone.0159434.

[65] M. Ušaj, K. Trontelj, D. Miklavčič, M. Kandušer, Cell-cell electrofusion: optimization of electric field amplitude and hypotonic treatment for mouse melanoma (B16-F1) and Chinese hamster ovary (CHO) cells, J. Membr. Biol. 236 (2010) 107–116, https://doi.org/10.1007/s00232-010-9272-3.

[66] S. Mesojednik, D. Pavlin, G. Serša, A. Coer, S. Kranjc, A. Grosel, G. Tevz, M. Čemažar, The effect of the histological properties of tumors on transfection efficiency of electrically assisted gene delivery to solid tumors in mice, Gene Ther. 14 (2007) 1261–1269, https://doi.org/10.1038/sj.gt.3302989.

[67] G.A. Meek, H.Y. Elder, Analytical and Quantitative Methods in Microscopy, CUP Archive, (1977).

[68] A. Maček Lebar, G. Serša, M. Čemažar, D. Miklavčič, Elektroporacija Electroporation, Med. Razgledi. (1998) 339–354.

[69] R. Shirakashi, V.L. Sukhorukov, I. Tanasawa, U. Zimmermann, Measurement of the permeability and resealing time constant of the electroporated mammalian cell membranes, Int. J. Heat Mass Transf. 47 (2004) 4517–4524, https://doi.org/10.1016/j.ijheatmasstransfer.2004.04.007.

[70] C.S. Djuzenova, U. Zimmermann, H. Frank, V.L. Sukhorukov, E. Richter, G. Fuhr, Effect of medium conductivity and composition on the uptake of propidium iodide into electropermeabilized myeloma cells, Biochim. Biophys. Acta Biomembr. 1284 (1996) 143–152, https://doi.org/10.1016/S0005-2736(96)00119-8.

[71] S. Čorović, L.M. Mir, D. Miklavčič, In vivo muscle electroporation threshold determination: realistic numerical models and in vivo experiments, J. Membr. Biol. 245 (2012) 509–520, https://doi.org/10.1007/s00232-012-9432-8.

[72] D. Šel, A.M. Lebar, D. Miklavčič, Feasibility of employing model-based optimization of pulse amplitude and electrode distance for effective tumor electropermeabilization, IEEE Trans. Biomed. Eng. 54 (2007) 773–781, https://doi.org/10.1109/TBME.2006.889196.

[73] J. Dermol, D. Miklavčič, Predicting electroporation of cells in an inhomogeneous electric field based on mathematical modeling and experimental CHO-cell permeabilization to propidium iodide determination, Bioelectrochemistry 100 (2014) 52–61, https://doi.org/10.1016/j.bioelechem.2014.03.011.

[74] M. Kranjc, S. Kranjc, F. Bajd, G. Serša, I. Serša, D. Miklavčič, Predicting irreversible electroporation-induced tissue damage by means of magnetic resonance electrical impedance tomography, Sci. Rep. 7 (2017) 10323, , https://doi.org/10.1038/s41598-017-10846-5.

[75] O. Tounekti, A. Kenani, N. Foray, S. Orlowski, Ll.M. Mir, The ratio of single- to double-strand DNA breaks and their absolute values determine cell death pathway, Br. J. Cancer 84 (2001) 1272–1279.

[76] G. Poste, J. Doll, I.R. Hart, I.J. Fidler, In vitro selection of murine B16 melanoma variants with enhanced tissue-invasive properties, Cancer Res. 40 (1980) 1636–1644.

[77] T.B. Napotnik, D. Miklavčič, In vitro electroporation detection methods – an overview, Bioelectrochemistry (2017), https://doi.org/10.1016/j.bioelechem.2017.12.005.

[78] J. Belehradek, S. Orlowski, L.H. Ramirez, G. Pron, B. Poddevin, L.M. Mir, Electropermeabilization of cells in tissues assessed by the qualitative and quantitative electroloading of bleomycin, Biochim. Biophys. Acta 1190 (1994) 155–163.

[79] P.E. Engström, B.R.R. Persson, L.G. Salford, Dynamic gamma camera studies of –bleomycin complex in normal and glioma bearing rats after in vivo electropermeabilization using exponential high-voltage pulses, Bioelectrochem. Bioenerg. 46 (1998) 241–248, https://doi.org/10.1016/S0302-4598(98)00141-X.

[80] G. Grafström, P. Engström, L.G. Salford, B.R.R. Persson, 99mTc-DTPA uptake and electrical impedance measurements in verification of in vivo electropermeabilization efficiency in rat muscle, Cancer Biother. Radiopharm. 21 (2006) 623–635, https://doi.org/10.1089/cbr.2006.21.623.

[81] D. Batiuškaitė, D. Cukjati, L.M. Mir, Comparison of in vivo electropermeabilization of normal and malignant tissue using the 51Cr-EDTA uptake test, Biol. Ther. Dent. (2003) (2003) 45–47.

[82] P.A. Garcia, J.H. Rossmeisl, J.L. Robertson, J.D. Olson, A.J. Johnson, T.L. Ellis, R.V. Davalos, 7.0-T magnetic resonance imaging characterization of acute blood-brain-barrier disruption achieved with intracranial irreversible electroporation, PLoS ONE 7 (2012) e50482, , https://doi.org/10.1371/journal.pone.0050482.

[83] M. Kranjc, B. Markelc, F. Bajd, M. Čemažar, I. Serša, T. Blagus, D. Miklavčič, In situ monitoring of electric field distribution in mouse tumor during electroporation, Radiology 274 (2015) 115–123, https://doi.org/10.1148/radiol.14140311.

[84] G. Serša, S. Kranjc, J. Ščančar, M. Kržan, M. Čemažar, Electrochemotherapy of mouse sarcoma tumors using electric pulse trains with repetition frequencies of 1 Hz and 5 kHz, J. Membr. Biol. 236 (2010) 155–162, https://doi.org/10.1007/s00232-010-9268-z.

[85] M. Ogihara, O. Yamaguchi, Potentiation of effects of anticancer agents by local electric pulses in murine bladder cancer, Urol. Res. 28 (2000) 391–397.

[86] M. Čemažar, D. Miklavčič, J. Ščančar, V. Dolžan, R. Golouh, G. Serša, Increased platinum accumulation in SA-1 tumour cells after in vivo electrochemotherapy with cisplatin, Br. J. Cancer 79 (1999) 1386–1391, https://doi.org/10.1038/sj.bjc.6690222.

[87] M. Čemažar, V. Todorovič, J. Ščančar, U. Lampreht, M. Štimac, U. Kamenšek, S. Kranjc, A. Coer, G. Serša, Adjuvant TNF-α therapy to electrochemotherapy with intravenous cisplatin in murine sarcoma exerts synergistic antitumor effectiveness, Radiol. Oncol. 49 (2015) 32–40, https://doi.org/10.1515/raon-2015-0005.

[88] R. Hudej, D. Miklavčič, M. Čemažar, V. Todorovič, G. Serša, A. Bergamo, G. Sava, A. Martinčič, J. Ščančar, B.K. Keppler, I. Turel, Modulation of activity of known cytotoxic ruthenium(III) compound (KP418) with hampered transmembrane transport in Electrochemotherapy in vitro and in vivo, J. Membr. Biol. 247 (2014) 1239–1251, https://doi.org/10.1007/s00232-014-9696-2.

[89] G. Pucihar, T. Kotnik, D. Miklavčič, J. Teissié, Kinetics of transmembrane transport of small molecules into Electropermeabilized cells, Biophys. J. 95 (2008) 2837–2848, https://doi.org/10.1529/biophysj.108.135541.

[90] J. Gehl, T. Skovsgaard, L.M. Mir, Enhancement of cytotoxicity by electropermeabilization: an improved method for screening drugs, Anti-Cancer Drugs 9 (1998) 319–325.

[91] V. Todorovič, G. Serša, K. Flisar, M. Čemažar, Enhanced cytotoxicity of bleomycin and cisplatin after electroporation in murine colorectal carcinoma cells, Radiol. Oncol. 43 (2009), https://doi.org/10.2478/v10019-009-0037-5.

[92] J.L. Vásquez, P. Ibsen, H. Lindberg, J. Gehl, In vitro and in vivo experiments on electrochemotherapy for bladder Cancer, J. Urol. 193 (2015) 1009–1015, https://doi.org/10.1016/j.juro.2014.09.039.

[93] Q. Chang, O.I. Ornatsky, I. Siddiqui, R. Straus, V.I. Baranov, D.W. Hedley, Biodistribution of cisplatin revealed by imaging mass cytometry identifies extensive collagen binding in tumor and normal tissues, Sci. Rep. 6 (2016), https://doi.org/10.1038/srep36641.

[94] W.J.F. van der Vijgh, I. Klein, Protein binding of five platinum compounds: comparison of two ultrafiltration systems, Cancer Chemother. Pharmacol. 18 (1986) 129–132, https://doi.org/10.1007/BF00262281.
[95] J.E. Melvik, J.M. Dornish, E.O. Pettersen, The binding of cis-dichlorodiammineplatinum(II) to extracellular and intracellular compounds in relation to drug uptake and cytotoxicity in vitro, Br. J. Cancer 66 (1992) 260–265, https://doi.org/10.1038/bjc.1992.254.
[96] K. Takahashi, T. Seki, K. Nishikawa, S. Minamide, M. Iwabuchi, M. Ono, S. Nagamine, H. Horinishi, Antitumor activity and toxicity of serum protein-bound platinum formed from cisplatin, Jpn. J. Cancer Res. Gann. 76 (1985) 68–74.
[97] P.A. Andrews, S. Velury, S.C. Mann, S.B. Howell, Cis-Diamminedichloroplatinum (II) accumulation in sensitive and resistant human ovarian carcinoma cells, Cancer Res. 48 (1988) 68–73.
[98] P. Workman, E.O. Aboagye, F. Balkwill, A. Balmain, G. Bruder, D.J. Chaplin, J.A. Double, J. Everitt, D.A.H. Farningham, M.J. Glennie, L.R. Kelland, V. Robinson, I.J. Stratford, G.M. Tozer, S. Watson, S.R. Wedge, S.A. Eccles, Guidelines for the welfare and use of animals in cancer research, Br. J. Cancer 102 (2010) 1555–1577, https://doi.org/10.1038/sj.bjc.6605642.
[99] S.M. Sancho-Martínez, L. Prieto-García, M. Prieto, J.M. López-Novoa, F.J. López-Hernández, Subcellular targets of cisplatin cytotoxicity: an integrated view, Pharmacol. Ther. 136 (2012) 35–55, https://doi.org/10.1016/j.pharmthera.2012.07.003.
[100] M. Nishikawa, M. Hashida, Pharmacokinetics of anticancer drugs, plasmid DNA, and their delivery systems in tissue-isolated perfused tumors, Adv. Drug Deliv. Rev. 40 (1999) 19–37, https://doi.org/10.1016/S0169-409X(99)00038-1.
[101] R. Susil, D. Šemrov, D. Miklavčič, Electric field induced transmembrane potential depends on cell density and organization, Electro Magnetobiol. 17 (1998) 391–399.
[102] M. Pavlin, N. Pavšelj, D. Miklavčič, Dependence of induced transmembrane potential on cell density, arrangement, and cell position inside a cell system, IEEE Trans. Biomed. Eng. 49 (2002) 605–612, https://doi.org/10.1109/TBME.2002.1001975.
[103] M. Essone Mezeme, G. Pucihar, M. Pavlin, C. Brosseau, D. Miklavčič, A numerical analysis of multicellular environment for modeling tissue electroporation, Appl. Phys. Lett. 100 (2012) 143701, , https://doi.org/10.1063/1.3700727.
[104] D. Miklavčič, M. Snoj, A. Županič, B. Kos, M. Čemažar, M. Kropivnik, M. Bračko, T. Pečnik, E.M. Gadžijev, G. Serša, Towards treatment planning and treatment of deep-seated solid tumors by electrochemotherapy, Biomed. Eng. Online 9 (2010) 10, https://doi.org/10.1186/1475-925X-9-10.
[105] A.I. Minchinton, I.F. Tannock, Drug penetration in solid tumours, Nat. Rev. Cancer 6 (2006) 583–592, https://doi.org/10.1038/nrc1893.
[106] J. Pušenjak, D. Miklavčič, Modeling of interstitial fluid pressure in solid tumor, Simul. Pract. Theory. 8 (2000) 17–24.
[107] L.J. Nugent, R.K. Jain, Extravascular diffusion in normal and neoplastic tissues, Cancer Res. 44 (1984) 238–244.
[108] P.F. Morrison, R.L. Dedrick, Transport of cisplatin in rat brain following microinfusion: an analysis, J. Pharm. Sci. 75 (1986) 120–128, https://doi.org/10.1002/jps.2600750204.
[109] G.M. Thurber, R. Weissleder, A systems approach for tumor pharmacokinetics, PLoS ONE 6 (2011) e24696, , https://doi.org/10.1371/journal.pone.0024696.
[110] A. Grošelj, M. Kržan, T. Kosjek, M. Bošnjak, G. Serša, M. Čemažar, Bleomycin pharmacokinetics of bolus bleomycin dose in elderly cancer patients treated with electrochemotherapy, Cancer Chemother. Pharmacol. (2016), https://doi.org/10.1007/s00280-016-3004-z.
[111] T. Kosjek, A. Krajnc, T. Gornik, D. Zigon, A. Grošelj, G. Serša, M. Čemažar, Identification and quantification of bleomycin in serum and tumor tissue by liquid chromatography coupled to high resolution mass spectrometry, Talanta 160 (2016) 164–171, https://doi.org/10.1016/j.talanta.2016.06.062.
[112] M. Čemažar, T. Jarm, D. Miklavčič, A. Maček Lebar, A. Ihan, N.A. Kopitar, G. Serša, Effect of electric-field intensity on electropermeabilization and electrosensitivity of various tumor-cell lines in vitro, Electro Magnetobiol. 17 (1998) 263–272.
[113] V. Sresht, J.R. Bellare, S.K. Gupta, Modeling the cytotoxicity of cisplatin, Ind. Eng. Chem. Res. 50 (2011) 12872–12880, https://doi.org/10.1021/ie102360e.
[114] J.-Y. Hong, G.-H. Kim, J.-W. Kim, S.-S. Kwon, E.F. Sato, K.-H. Cho, E. Shim, Computational modeling of apoptotic signaling pathways induced by cisplatin, BMC Syst. Biol. 6 (2012) 122, https://doi.org/10.1186/1752-0509-6-122.
[115] A.W. El-Kareh, T.W. Secomb, A mathematical model for cisplatin cellular pharmacodynamics, Neoplasia 5 (2003) 161–169, https://doi.org/10.1016/S1476-5586(03)80008-8.
[116] P.D. Sadowitz, B.A. Hubbard, J.C. Dabrowiak, J. Goodisman, K.A. Tacka, M.K. Aktas, M.J. Cunningham, R.L. Dubowy, A.-K. Souid, Kinetics of cisplatin binding to cellular DNA and modulations by thiol-blocking agents and thiol drugs, Drug Metab. Dispos. Biol. Fate Chem. 30 (2002) 183–190.